Heparan Sulfate Proteoglycan Synthesis is Dysregulated in Human Osteoarthritic Cartilage.

Anastasios Chanalaris[*], Hannah Clarke[†], Scott E. Guimond[†], Tonia L. Vincent[*], Jeremy E. Turnbull[†], Linda Troeberg[*, ††]

[*] Arthritis Research UK Centre for Osteoarthritis Pathogenesis, Kennedy Institute of Rheumatology, University of Oxford, Roosevelt Drive, Oxford, OX3 7FY, UK

[†] Institute of Integrative Biology, University of Liverpool, Crown Street, Liverpool, L69 7ZB, UK

[††] Norwich Medical School, BCRE, University of East Anglia, Norwich, NR4 7TJ, UK

Number of text pages: 32; number of tables: 1 (+1 Supplementary); number of figures: 6.

Running title: Heparan sulfation altered in osteoarthritis

Supported by: This work was supported by Arthritis Research UK grants 20887, 20205 and 21621 and by the National Institute for Health Research (NIHR) Oxford Biomedical Research Centre (BRC). Disclaimer: The views expressed are those of the author(s) and not necessarily those of the NHS, the NIHR or the Department of Health.

Address correspondence to: Linda Troeberg, Ph. D., Arthritis Research UK Centre for Osteoarthritis Pathogenesis, Kennedy Institute of Rheumatology, University of Oxford, Roosevelt Drive, Oxford, OX3 7FY, UK. E-mail: linda.troeberg@kennedy.ox.ac.uk

Conflict of interest: All authors declare that there is no conflict of interest regarding this study.

Abbreviations: ACLT, anterior cruciate ligament transection; ADAMTS, adamalysin with thrombospondin motifs; BKY, Benjamini, Krieger and Yekutieli; BMP, bone morphogenetic protein; CTGF, connective tissue growth factor; DMM, destabilisation of the medial meniscus; ERK,

29 extracellular signal-regulated kinase; FGF2, fibroblast growth factor 2; GlcA, glucuronic acid; GLCE
30 glucuronyl C5-epimerase; GlcNAc, N-acetyl glucosamine; GlcNS, *N*-sulfoglucosamine; HS, heparan
31 sulfate; GPC, glypican; HSPG2, perlecan; IdoA, iduronic acid; MMP, matrix metalloproteinase; NDST,
32 N-deacetylase/N-sulfotransferase; OA, osteoarthritis; SDC, syndecan; TGFβ, transforming growth
33 factor β; TIMP, tissue inhibitor of metalloproteinases; UA, uronic acid, 2S, 2-O-sulfate; 6S, 6-O-
34 sulfate.

Abstract

Osteoarthritis (OA) is a common degenerative joint disease, characterised by cartilage loss and subchondral bone remodelling in response to abnormal mechanical load. Heparan sulfate (HS) proteoglycans bind to many proteins that regulate cartilage homeostasis, including growth factors, morphogens, proteases and their inhibitors, and modulate their localization, retention and biological activity. Changes in HS expression and structure may thus have important consequences for joint health. We analysed normal and osteoarthritic human knee cartilage, and found HS biosynthesis was markedly disrupted in OA, with 45% of the 38 genes analysed differentially regulated in diseased cartilage. Expression of several HS core proteins, biosynthesis and modification enzymes was increased in OA cartilage, while expression of the HS proteoglycans syndecan 4 and betaglycan was reduced. The structure of HS was also altered, with increased levels of 6-O-sulfation in osteoarthritic samples. This correlated with increased expression of *HS6ST1*, a 6-O-sulfotransferase, and *GLCE*, an epimerase that promotes 6-O-sulfation. siRNA silencing of *HS6ST1* expression in primary OA chondrocytes inhibited ERK phosphorylation in response to FGF2, showing that changes in 6-O-sulfation impact a key cartilage signalling pathway. Given the broad range of homeostatic and repair pathways that HS regulates, these changes in proteoglycan expression and HS structure are likely to have significant effects on joint health and progression of osteoarthritis.

Introduction

Osteoarthritis (OA) is a common degenerative joint disease in which articular cartilage loss and subchondral bone remodelling cause pain and impair movement of affected joints. There are currently no disease-modifying therapies available, and patients are largely treated with analgesia or joint replacement surgery. There is thus a substantial need to develop effective therapeutics that can slow or halt the progression of joint damage.

The primary risk factors for development of OA are ageing and injury, which alter the mechanical environment of the joint and stimulate chondrocytes to produce catabolic proteinases that degrade the cartilage extracellular matrix. The pericellular matrix immediately adjacent to chondrocytes is thought

63 to play a central role in transducing mechanical stimuli to biochemical signals within the cells.[1] For
64 example, loading of cartilage causes release of fibroblast growth factor 2 (FGF2) from the pericellular
65 matrix, and activates downstream extracellular signal-regulated kinase (ERK) signalling pathways in
66 chondrocytes.[2, 3] FGF2 is localized in the pericellular matrix through its interaction with the heparan
67 sulfate (HS) chains of perlecan,[2] the major HS proteoglycan in cartilage. Pericellular matrix and cell
68 surface HS also binds to a large number of other bioactive proteins, including growth factors [e. g.
69 connective tissue growth factor (CTGF) and transforming growth factor β (TGFβ)], morphogens [e. g.
70 bone morphogenetic protein (BMP)-4 and BMP-7], proteinases [e. g. matrix metalloproteinase 13
71 (MMP-13), adamalysin with thrombospondin motifs 4 (ADAMTS-4), and ADAMTS-5] and proteinase
72 inhibitors (e. g. tissue inhibitor of metalloproteinases, TIMP-3), and regulates their retention,
73 localization and biological activity.[4, 5] HS is thus a critical regulator of chondrocyte homeostasis and
74 cartilage health. Previous studies have shown increased expression of some of the HS core proteins in
75 OA, including perlecan,[6-9] syndecan 1[9-11] and syndecan 4,[11-13] but nothing is yet known about how the
76 structure of HS itself or its interactions with ligands changes in OA.
77 HS interacts with proteins through electrostatic interactions between its negatively charged sulfate
78 groups and positively charged lysine and arginine residues on the protein ligand. The number and
79 arrangement of sulfate groups along the HS glycosaminoglycan chain determines the affinity of HS for
80 its protein ligands and its ability to modulate their biological activity.[14-16] This sulfation pattern is
81 generated by the template-independent action of a series of sulfotransferases during HS synthesis in the
82 Golgi apparatus.[17] The EXT family of glycosyltransferases initiate HS synthesis by adding sequential
83 glucuronic acid (GlcA) and N-acetyl glucosamine (GlcNAc) residues to a linker tetrasaccharide
84 attached to the core protein. GlcA can subsequently be epimerized to iduronic acid (IdoA) by glucuronyl
85 C5-epimerase (GLCE). The growing HS chain can then be N-sulfated on GlcNAc residues [by the N-
86 deacetylase/N-sulfotransferases (NDSTs)], and/or O-sulfated on GlcNAc [by the 6-O-sulfotransferases
87 (HS6STs) and 3-O-sulfotransferases (HS3ST)] and GlcA/IdoA [by the 2-O-sulfotransferase
88 (HS2ST1)].[17] HS can also be edited in the extracellular environment by SULF1 and SULF2 that remove
89 6-O-sulfate groups, or degraded by the heparanases HSPE1 and HSPE2. These reactions do not always
90 occur to completion, generating a highly variable sulfation pattern that gives HS a structural complexity

several orders of magnitude larger than the proteome. Temporal and spatial changes in HS sulfation occur during development[18-21] and in diseases such as Alzheimer's disease[22, 23], cancer,[24] diabetes,[25] and fibrosis,[26] and are thought to enable HS to coordinately regulate the retention and activity of multiple bioactive ligands, and thus to powerfully regulate tissue homeostasis.

Here, we isolated RNA from knee cartilage of normal and osteoarthritic donors, and profiled expression of the 13 core proteins and 25 biosynthesis and modifying enzymes that govern HS structure and sulfation. Notably, we also undertook the first examination of disaccharide composition by isolating HS from normal and OA cartilage. This showed that HS enzyme expression and glycan structure are markedly dysregulated in OA cartilage, and identifies increased 6-O-sulfation of HS as the primary structural change associated with impaired cartilage homeostasis.

Materials and Methods

Human cartilage samples

Human articular cartilage was obtained in full compliance with national and institutional ethical requirements, the United Kingdom Human Tissue Act, and the Declaration of Helsinki.

Normal human knee cartilage specimens used for RNA and glycosaminoglycan analyses were obtained from Articular Engineering LLC (Illinois, USA) from donors (6 females of 44-68 years old, 6 males of 32-75 years old) with clinically healthy, normal cartilage and no history of OA, following informed donor consent and approval by local ethics committees and the University of Oxford Research Ethics Committee (R45926/RE001). Cartilage was aseptically harvested within 48 hours of death, flash frozen in liquid nitrogen, stored at -80^{o}C, and shipped in dry ice.

Normal human knee cartilage specimens used for immunohistochemistry were obtained from Stanmore Biobank (Royal National Orthopaedic Hospital, Stanmore) from donors undergoing amputation for low limb malignancies with no involvement of the cartilage, following informed donor consent and approval by the Royal Veterinary College Ethics and Welfare Committee (Institutional approval Unique Reference Number 2012 0048H). Cartilage was aseptically harvested from all surfaces

of the joint within 4 hours of surgery and processed for downstream analyses.

Human OA cartilage samples used for immunohistochemistry, RNA and glycosaminoglycan analyses were obtained from the Oxford Musculoskeletal Biobank from donors (6 females of 58-83 years old, 6 males of 52-84 years old) undergoing total knee replacement surgery for advanced OA, following informed consent and approval by the Oxford Research Ethics Committee C (09/H0606/11). Cartilage was aseptically harvested from all surfaces of the joint within 4 hours of surgery and processed for downstream analyses.

RNA isolation

Cartilage (300 mg) from 12 normal and 12 OA donors was ground under liquid nitrogen with a pestle and mortar. The ground cartilage powder was added to 1.5 ml of RLT lysis buffer supplemented with 10 µl/ml β-mercaptoethanol (QIAGEN, UK), digested with proteinase K (6-10 mAU/100 mg of cartilage, 10 min at 55°C, QIAGEN, UK) and transferred to an RNeasy micro column (QIAGEN, UK). RNA was extracted according to the manufacturers' protocol with an intermediate DNA digestion step. The eluted RNA was quantified on a Nanodrop spectrophotometer and examined on a Bioanalyser (Agilent, UK). RNA from healthy and OA cartilage had comparable RINs (6-7.7) and RNA yields.

Reverse transcription and quantitative PCR

Total RNA (250 ng) was reverse transcribed to cDNA using a reverse transcription kit (ThermoFisher) and cDNA amplified on a Taqman low density array (Table 1). Fold changes against the control samples were calculated using the ΔΔCt method. For calculating the ΔCt, the average of the three normalising genes (18S, RLPL0, GAPDH) was used.

Extraction of HSPGs and disaccharide analysis

Approximately 300 mg of frozen cartilage explants were ground in a pestle and mortar under liquid

nitrogen and the powder was placed in 1 ml of Trizol (ThermoFisher Scientific, UK). After phase separation with the addition of chloroform, the aqueous phase was added to equilibrated DEAE-Sephacel beads, washed with PBS and 0.25 M NaCl before elution with 2 M NaCl. The eluate was desalted on PD10 columns and freeze dried. The samples were then treated with DNase (QIAGEN, UK) and RNase, prior to incubation with chondroitinase ABC (Sigma Aldrich, UK), neuraminidase, keratanase and pronase. Following the digestions, the samples were once more purified on DEAE beads and freeze dried. The rest of the procedure was as described before.[27] Briefly, samples were sequentially digested with heparanase I, II and III (IBEX Technologies, UK), purified on C18 and graphite spin columns (ThermoFisher Scientific, UK) and labelled with BIODIPY hydrazine (ThermoFisher Scientific, UK) as previously described.[28] Finally, samples underwent ethanol precipitation to remove any copurified impurities. Samples were then analysed by SAX HPLC using a Propac PA-1 strong anion-exchange column (4.6x250nm; Dionex, UK). Samples were eluted with a linear gradient of 0-1 M sodium chloride and isocratic sodium hydroxide (150 mM) over 30 min at 1 ml/min on a Shimadzu HPLC system. An inline fluorimeter was used to detect eluted peaks (excitation λ = 488 nm, emission λ = 520 nm). Previously calculated correction factors were applied to quantitate the observed disaccharides.[27]

Immunofluorescence staining analysis

Upon receipt, cartilage explants were embedded in OCT (Thermofisher Scientific, UK) and frozen in isopentane for storage at -80°C until sectioning. Samples were mounted on a cryostat (CM1860UV, Leica, Milton Keynes, UK) and 5 μm sections were cut and mounted on Superfrost Plus microscope slides (ThermoFisher Scientific, UK) and stored at -80 °C. Frozen sections were air dried for 1 hour at room temperature and fixed with neutral buffered formalin for 5 minutes at room temperature prior to their incubation in ice cold acetone for 10 minutes at -20 °C, and incubated at 37 °C for 30 minutes with 0.1 U chondroitinase ABC (Sigma, C3667) in 1x chondroitinase buffer (40 mM Tris-acetate, pH 8). The digested sections were blocked in 1% goat serum and 5% BSA in PBS for 1 hour at room temperature. After 15 minutes permeabilization with 0.1% Triton X-100 in PBS, sections were washed

in PBS and the primary antibodies were applied diluted in block buffer overnight at 4°C, or isotype antibodies as negative controls. The following antibodies were used: rat anti-perlecan (HSPG2) (1:1000, Millipore, UK), rabbit anti-GLCE (1:20, HPA04821, Atlas Antibodies, Sweden), rabbit anti-EXTL2 (1:100, NBP2-16394, Novus, UK), mouse anti-NDST1 (3 µg/ml, ab55296, Abcam, UK), rabbit anti-GPC1 (1:250, HPA303571, Sigma, UK) and rabbit anti-HS6ST1 (1:250, ab106195, Abcam, UK). After washing in PBS at room temperature, the appropriate secondary antibodies were added; either in combination, or in unison, goat anti-rat Alexa Fluor 488 (1:1000, Thermo Fisher Scientific, UK), goat anti-rabbit Alexa Fluor 568 (1:500, Thermo Fisher Scientific, UK), or goat anti-mouse Alexa Fluor 568 (1:500, Thermo Fisher Scientific, UK) in block buffer. The secondary antibodies were washed off with PBS after 3 hours at room temperature. Nuclei were stained with DAPI (1:200 in PBS, Thermo Fisher Scientific, UK) for 1 hour before a final wash in PBS and mounting in Prolong Diamond antifade (Thermo Fisher Scientific UK).

Sections were viewed under an Olympus BX51 fluorescent microscope (Olympus, UK). For each protein the optimal duration of exposure was determined as that giving a signal in positively stained sections and no detectable staining in negatively stained sections, and avoiding overexposure and signal saturation. The exposures used were: HSPG2 200-250 ms, EXTL2 125 ms, GLCE 200 ms, GPC1 125 ms, NDST1 280-300 ms and HS6ST1 275-300ms. Images were obtained from at least 6 random regions of the cartilage under a 40x lens and then analysed on ImageJ as described previously.[29, 30] For representative images, the intensity of the red and green signal was adjusted for illustrative purposes. For quantification, raw unaltered images were analysed.

Analysis of ERK phosphorylation in chondrocytes

Primary OA chondrocytes were isolated from freshly harvested human OA cartilage by chopping the tissue finely and incubating in DMEM with 10% fetal calf serum (Gibco/ThermoFisher Scientific, UK) and 1.5 mg/ml type II collagenase (Roche, Switzerland)(18 hours, 37 °C, with shaking at 180 rpm). The suspension was passed through a cell strainer, pelleted and washed twice with medium. Isolated chondrocytes were cultured for 7 days until confluent[31] and stored at -80 °C until required. For small

interfering RNA (siRNA) transfection, chondrocytes ($3x10^5$/well) were transfected with 20 nM of either Silencer Select Negative control #1 or Silencer Select *HS6ST1* siRNA (s17978, Ambion/ThermoFisher Scientific, UK) using Lipofectamine 2000 (Gibco/ThermoFisher Scientific, UK) in serum free Opti-MEM I (ThermoFisher Scientific).[31] After 4 hours, the medium was replaced with DMEM containing 10% FCS and cell cultured for a further 72 hours.

To analyse ERK phosphorylation, siRNA-treated chondrocytes were cultured in serum-free DMEM for 24 hours, and treated with PBS recombinant human FGF2 (R&D Systems, USA)(20 ng/ ml, 10 min). Cells were then washed twice with ice-cold PBS and lysed on ice in RIPA buffer (150 µl) containing protease inhibitors (SIGMAFAST, Sigma-Aldrich, UK) and phosphatase inhibitors (20mM NaF, 100 mM Na_3VO_4, 100 mM beta-glycerophosphate, 100 mM sodium pyrophosphate). Lysates were centrifuged (5000 rpm, 3 min) and 20 µg of protein analysed by immunoblotting using antibodies against phosphoERK1/2 (1:2500, E7028, Sigma-Aldrich, UK) and total ERK (1:5000, 4695S, Cell Signalling Technology, UK) in block buffer (5% milk/PBST). After 3x 5 min washes with PBST, the membranes were incubated with an AP-conjugated anti-rabbit secondary antibody (1:2000, Promega, UK) and developed using Western Blue stabilized substrate (Promega, UK). Immunoblots were analysed by densitometry using Phoretix 1D software (TotalLab, Newcastle-upon-Tyne, UK) and the levels of phospho-ERK normalised to total ERK for each treatment, and expressed relative to the corresponding untreated sample (defined as 1).

Efficacy of siRNA silencing was confirmed by isolating RNA from RIPA lysates (20 – 50 µl, diluted to 350 µl with RLT buffer containing 1% v/v β-mercaptoethanol) using RNeasy micro kits according to the manufacturer's protocol (QIAGEN, Germany). Isolated RNA was reverse transcribed and expression of *18S*, *GAPDH* and *HS6ST1* quantified as described above.

Statistical analysis

All statistical tests, except correlations and linear regression models, were performed in Graphpad Prism version 7.0d. All other statistical tests were performed in R. All significant changes are annotated in the figures.

Power calculations were based on pilot data from 4 samples per group. According to the pilot experiments, we calculated the sample size required for a two-tailed t-test with an effect size of 1.5 (difference between means of 0.6 and standard deviation of 0.4) and type I error rate α at 5%, to be 12 samples per group. Therefore we extended the groups to the appropriate sizes.

Prior to performing any parametric test, groups were tested for normality using the D'Agostino and Pearson omnibus test.[32]

We performed two-way ANOVA and examined the forest plots (Figure 1) to evaluate whether there was significant variation in the age or sex of the donors.

All tests on the PCR results were performed on the ΔΔCt values as they were normally distributed. Multiple two-tailed t-tests were performed, comparing the expression of each gene between the two groups. The derived p-values were corrected for multiplicity using the two-stage step-up method of Benjamini, Krieger and Yekutieli (BKY), with a false discovery rate cut-off at 5%.[33]

For HS disaccharide composition, site of sulfation and extent of sulfation, two-way ANOVA was performed, with a BKY multiplicity correction.

Hierarchical clustering was performed in R (https://www.r-project.org) using the package gplots ßand RColorBrewer. Canberra distance was employed as the clustering metric.

For analysis of immunofluorescence images, the background-corrected integrated intensity values per cell were aggregated for the normal and OA groups (n = 3-6 per group), and the cumulative distributions of signal were analysed using the Kolmogorov-Smirnov test, since the values were not normally distributed.

Results

Expression of HS proteoglycan core proteins was disrupted in OA cartilage

We isolated RNA from normal and osteoarthritic tibial knee cartilage (n = 12 per group), and examined expression of 13 genes encoding HS proteoglycan core proteins. Genes with a significant change in expression are shown in Figure 1.

Expression of agrin (*AGRN*) and perlecan (*HSPG2*) was significantly increased in OA samples (multiple t-tests, BKY corrected q>0.05), while expression of betaglycan (TGF β receptor III, *TGFBR3*) was reduced.

Among the syndecan family, syndecan 2 (*SDC2*) was not differentially regulated between the groups, while expression of syndecan 4 (*SDC4*) was reduced in OA, and expression of syndecan 1 (*SDC1*) and syndecan 3 (*SDC3*) was increased. *SDC1* was the most strongly regulated of the HS core proteins, with mean expression increased 17-fold in OA.

Glypican core proteins showed fewer changes in expression in OA cartilage, with only glypican 1 (*GPC1*) showing significantly higher expression in OA samples. Expression of glypican 4 (*GPC4*), glypican 5 (*GPC5*) and glypican 6 (*GPC6*) was not significantly regulated, and glypican 2 (*GPC2*) and glypican 3 (*GPC3*) were minimally expressed in both normal and OA cartilage.

Expression of HS biosynthesis and modifying enzymes was also disrupted in OA cartilage

Using the same samples, we analysed expression of 25 genes encoding HS biosynthesis and modifying enzymes (Figure 1), and found that 10 of these were expressed at higher levels in OA cartilage.

Expression of *EXT1* and *EXT2*, which extend the growing HS chain, was increased in OA, as was expression of the related *EXTL1* and *EXTL2* genes. *EXTL1* was the most strong regulated of all the genes examined, showing a 24-fold increase in expression in OA. Expression of *EXLT3* was not significantly regulated. Mean expression of epimerase (*GLCE*), which epimerizes glucuronic acid (GluA) to iduronic acid (IdoA), was increased 2-fold in OA cartilage.

Mean expression of the N-sulfotransferase *NDST1* was 3-fold higher in OA cartilage. *NDST2* was expressed at similar levels in both sample groups, and *NDST3* and *NDST4* were not appreciably expressed in either normal or OA cartilage.

Expression of the 2-O-sulfotransferase *HS2ST1* was not significantly altered in OA samples. Of the 7 isoforms of 3-O-sulfotransferase, only *HS3ST1* showed increased expression in OA cartilage, with expression of *HS3ST3A1* and *HS3ST3B1* not differentially regulated and 4 of the isoforms (*HS3ST2*, *HS3ST3*, *HS3ST5*, *HS3ST6*) not detectably expressed in cartilage. Among the 3 6-O-sulfotransferases

isoforms, expression of *HS6ST1* was increased in OA cartilage, while *HS6ST3* expression was similar in both sample groups and *HS6ST2* was expressed at low levels.

Expression of both *SULF1* and *SULF2* was increased in OA cartilage, with *HSPE* and *HSPE2* not differentially expressed.

Cluster analysis of the samples, based on the levels of the significantly regulated genes, separated the samples into two clusters (Figure 2), with the first cluster containing all the OA samples and one of the normal samples, and the second cluster containing the remaining normal samples. This indicates that levels of expression of the 17 significantly regulated genes are largely able to discriminate normal and osteoarthritic cartilage.

Selected immunohistochemical analyses validate observed changes in expression

In order to establish whether the gene regulation we observed resulted in corresponding changes in protein expression, we selected six proteins (HSPG2, EXTL2, GLCE, NDST1, HS6ST1 and GPC1) to analyse by semi-quantitative immunofluorescence staining on frozen sections of normal and OA cartilage. We selected HSPG2 as a marker of pericellular matrix localisation, and the other 5 proteins according to functional antibody availability and in order to have at least one from each category of HS core proteins and biosynthetic enzymes. The intensity of staining did not vary with cartilage depth for any of the antibodies examined.

As expected, HSPG2 exhibited a predominantly pericellular localization,[34] with approximately 50% increased expression per cell in the 4 OA samples we examined compared to the 6 normal cartilage samples.

EXTL2 had a predominantly perinuclear localization in both normal and OA cartilage (Figure 3A). In OA cartilage, expression of EXTL2 was increased 1.6-fold, with a decrease in the number of cells not expressing EXTL2 and a shift towards more cells expressing moderate amounts of the protein (Figure 3B).

GLCE was similarly localized in the perinuclear region of cells (Figure 3C), with 2.4-fold higher expression in OA and a shift towards more cells expressing modest amount of the enzyme (Figure 3D).

HS6ST1 intensity levels were approximately 3 times higher in OA (Figure 4B). The protein appeared to be expressed at low levels around the nucleus in normal cartilage and to show some pericellular staining in the OA samples (Figure 4A).

NDST1 was localized in the perinuclear region in normal cells, with more expression towards the periphery of the cell and overlapping with HSPG2 in the OA samples (Figure 4C). Intensity levels were approximately 3.6-fold higher in the OA samples (Figure 4D).

Staining for GPC1 was predominantly intracellular (Figure 5A), with 5.5-fold higher intensity in OA samples (Figure 5B).

Increased 6-O-sulfation of HS in OA cartilage

We analyzed the amount and disaccharide composition of HS isolated from normal and OA cartilage (n = 8 per group, Figure 6A).

There was no significant difference in the total amount of HS in the normal and OA cartilage samples (5.7 ± 2.3 μg/100 mg in the normal samples, 3.0 ± μg/100 mg of tissue in OA, P >0.05 by t-test, Figure 6B), or in the ratio of sulfated to total HS disaccharides (36.5 % in normal cartilage, 53% in OA cartilage, Mann Whitney test, P >0.05, Figure 6C).

Normal and OA cartilage did not differ significantly in the abundance of any single HS disaccharide (Figure 6D), or in the percentages of non-, mono-, di or triple- sulfated disaccharides (not shown). However, the percentage of 6-O-sulfated disaccharides was increased in OA cartilage (19.8% vs 12.1%, Mann Whitney test, P = 0.0379, Figure 6E).

6-O-sulfation of HS correlated with expression of GLCE, HS6ST1, EXTL2 and HS3ST3A1

We examined whether expression of any of HS biosynthesis genes correlated with the HS disaccharide compositions quantified.

The percentage of 6-O-sulfated disaccharides correlated with expression of *HS6ST1* (r = 0.74, p = 0.0016, Figure 6F), *GLCE* (r = 0.775, p = 0.0007, Figure 6G), *EXTL2* (r = 0.57, p = 0.026), and

HS3ST3A1 (r = 0.575, p = 0.025). The relationship between 6-O-sulfation and *HS6ST1* expression was linear, with a 4% increase in abundance of 6-O-sulfated disaccharides for every doubling in the amount of *HS6ST1* (adjusted $R^2 = 0.525$, p = 0.0014). This relationship was independent of age, OA and gender. The relationship between 6-O-sulfation and *GLCE* expression was linear, with a doubling in expression of GLCE increasing the percentage of 6-O-sulfation by about 4%. This relationship was dependent on age and gender, such that for every year increase in age there was a 0.17% increase in % 6-O-sulfation, and that females had about 4% more 6-O-sulfation for the same amount of GLCE (adjusted $R^2 = 0.42$, p = 0.028).

The percentage of 2-O-sulfated disaccharides correlated with expression of *HS3ST3A1* (r = 0.796, p = 0.0004) and *HS6ST1* (r = 0.57, p = 0.026). The relationship between 2-O-sulfation and *HS3ST3A1* expression was linear, with a doubling in the levels of *HS3ST3A1* increasing the percentage of 2-O-sulfated disaccharides by 4%. This association was OA- and gender-dependent, such that females with OA had a 0.62% increase in 2-O-sulfation for the same level of *HS3ST3A1*expression (adj $R^2 = 0.67$, p = 0.0036).

We also examined correlations between expression of HS biosynthesis genes and the relative abundance of individual disaccharide residues. This showed that *HS3ST3A1* expression correlated with the percentage of UA(2S)-GlcNAc (r = 0.772, $P < 0.05$), UA(2S)-GlcNS (r = 0.538, $P < 0.05$) and UA-GlcNS(6S) (r = 0.521, $P < 0.05$), while *HS6ST1* expression correlated with the percentage of UA(2S)-GlcNAc (r = 0.53, $P < 0.05$), UA-GlcNAc(6S) (r = 0.58, $P < 0.05$) and UA-GlcNAc (r = -0.686, $P = 0.005$).

Finally, we found that *HS3ST2* expression was linearly associated with age, independent of OA and gender, with expression of *HS3ST2* increasing by 6-21% every year (adj $R^2 = 0.341$, p = 0.035).

siRNA silencing of HS6ST1 inhibits FGF2 signalling

To investigate whether changes in HS6ST1 expression and 6-O-sulfation have the capacity to alter signalling in OA chondrocytes, we isolated chondrocytes from knee cartilage of 5 donors with late-stage OA, and examined FGF2-dependent ERK phosphorylation after siRNA knockdown of *HS6ST1*.

siRNA treatment suppressed *HS6ST1* mRNA levels by >90% in all 5 donors (Figure 6H). Addition of 20 ng/ml FGF-2 stimulated rapid phosphorylation of ERK, and this was significantly reduced (by 40%) in *HS6ST1*-silenced cells (Figure 6I).

Discussion

HS proteoglycans control the retention, localization and biological activity of over 400 bioactive molecules, including growth factors (e. g. FGF2, TGFβ), morphogens (e. g. BMP-4, BMP-7), proteinases (e. g. MMP-13, ADAMTS-4, ADAMTS-5) and proteinase inhibitors (e. g. TIMP-3).[4, 35-37] Many HS ligands have significant impacts on cartilage homeostasis, making HS a critical regulator of joint health. Despite this important role, nothing was previously known about how the structure and sulfation pattern of HS may change during the development of osteoarthritis. Here, we report that expression of HS biosynthesis and modifying enzymes and the resulting HS disaccharide composition differs significantly in normal and osteoarthritic human knee cartilage.

Expression of the HS polymerases *EXT1* and *EXT2*, as well as *EXTL1* and *EXTL2*, was significantly increased in OA cartilage. The roles of these enzymes in homeostasis of adult cartilage has not been explored, but EXT1 and EXT2 are known to be important in musculoskeletal development. EXT1 regulates Ihh signalling during endochondral ossification,[38] and mutations in both EXT1 and EXT2 are associated with development of hereditary multiple exostoses, an inherited pediatric disorder characterised by osteochondroma formation.[39] Aberrant activation of chondrocyte hypertrophy has been implicated in development of OA,[40] and may underlie the elevated expression of *EXT1* and *EXT2* we observed. The role of the related *EXTL* genes in HS synthesis are less well understood, but they are thought to regulate early stages of HS chain elongation.[41] Mutations in EXTL3 have been shown to impair musculoskeletal development,[42] and while *EXTL3* expression was not regulated in OA, expression of both *EXTL1* and *EXTL2* was strongly upregulated.

Once polymerised, the HS chain can be modified by epimerisation of GlcA to IdoA by a glucuronyl epimerase (GLCE), or by addition of sulfate groups to specific positions in the disaccharide units, by multiple sulfotransferases. We measured expression of the 11 human HS sulfotransferases, and found

399 that expression of *NDST1*, *HS3ST1* and *HS6ST1* was elevated in OA cartilage. Most notably, we found
400 a significant increase in the level of 6-O-sulfated disaccharides in OA cartilage, which correlated
401 strongly with expression of both *HS6ST1* and *GLCE*. Epimerisation of GlcA to IdoA by GLCE is
402 thought to favour subsequent 6-O-sulfation,[43] suggesting that these two enzymes drive the increase in
403 6-O-sulfation in OA cartilage. Previous studies have shown that levels of 6-O-sulfation are spatially
404 and temporally regulated during development,[18, 19, 21] and in diseases such as fibrosis,[44, 45] Alzheimer's
405 disease,[22] and cancer.[46, 47] In the case of fibrosis, a doubling in 6-O-sulfation is thought to exacerbate
406 disease by amplifying TGFβ[44] and FGF-2[45] signaling. We hypothesized that increased 6-O-sulfation in
407 OA cartilage may similarly amplify downstream signalling pathways and alter tissue homeostasis.
408 Consistent with this, using primary OA chondrocytes isolated from 5 different donors, we found that
409 siRNA silencing of *HS6ST1* suppressed ERK phosphorylation in response to FGF2. This is in line with
410 previous studies showing that 6-O-sulfation of HS promotes FGF2 signalling,[48-51] and confirms that
411 changes in 6-O-sulfation can alter biologically relevant signalling pathways in cartilage. 6-O-sulfation
412 is known to alter HS affinity for a range of ligands,[52] with varying effects on their downstream activity.
413 For example, 6-O-sulfation promotes TGFβ[53, 54] signalling, and inhibits Wnt[55, 56] and BMP[57, 58]
414 signalling. An unbiased approach such as phosphoproteomics will be required to identify pathways
415 regulated by 6-O-sulfation in normal and OA cartilage.

416 The importance of 6-O-sulfation is underscored by the fact that it is the only HS modification that
417 is regulated at both the 'on' and the 'off' level, being added during HS biosynthesis in the Golgi
418 apparatus by HS6ST1, HS6ST2 and/or HS6ST3[43] and removed in the extracellular environment by the
419 6-O-endosulfatases SULF1 and/or SULF2.[59] This permits "remodelling" of HS sulfation that is
420 apparently critical to regulation of its functions. Indeed, we observed increased expression of SULF1
421 and SULF2 in OA cartilage, in line with previous reports examining both human and murine OA
422 cartilage.[7, 9, 11, 58, 60, 61] Despite this, net levels of 6-O-sulfation were increased in our OA cartilage
423 samples. As noted in recent studies from HS in muscle,[27] this highlights the importance of analysing
424 HS structure directly, and may indicate post-translational regulation of HS6ST and/or SULF activity,
425 or differences in the catalytic efficiency, location or stability of the enzymes. *Sulf1*$^{-/-}$ and *Sulf2*$^{-/-}$ mice
426 developed accelerated OA and injection of recombinant SULF1 into the joint reduced cartilage

damage,[62] indicating the enzymes play a chondroprotective role. This suggests that elevated 6-O-sulfation may contribute to or perpetuate cartilage damage, potentially through driving anabolic pathways or impairing catabolic repair mechanisms.

We did not find any increase in N-sulfation in OA cartilage, despite increased expression of NDST1 at the mRNA and protein level. We did not quantify the abundance of 3-O-sulfated disaccharides due to their relative scarcity, but expression of *HS3ST1* was elevated in OA samples. Further investigation may be warranted as knowledge of the functional impact of 3-O-sulfation and the extent of the 3-O-proteome expands.[63, 64]

With regards the HS core proteins, we observed the previously reported increase in expression of HSPG2[6-9], glypican 1,[11] syndecan 1[9-11] and syndecan 3[65] in OA cartilage, but not the previously observed increase in syndecan 4[9, 11-13] or decrease in agrin.[66] This may suggest species- or joint-specific variation in expression of these genes. Additionally, we observed that expression of many HS-associated genes was significantly altered by isolation and culture of chondrocytes (data not shown), suggesting that HS biosynthesis is dynamically regulated by the chondrocyte microenvironment and that expression may change during the course of OA development.

We observed a significant reduction in expression of TGFBR3 in OA cartilage. This HS core protein, also known as beta-glycan, does not have the ability to signal directly, but promotes TGFβ signalling by recruiting the growth factor and presenting it to the type II TGFβ receptor. In chondrocytes, TGFBR3 was recently shown to promote activation of latent TGFβ in a CTGF- and HS-dependent manner.[67] Reduction in expression of TGFBR3 in OA is thus likely to impair the chondroprotective effects of TGFβ signalling.

Previous rodent microarray studies indicate that expression of some HS core proteins, biosynthesis and modifying enzymes is regulated early in the course of OA development.[7, 8, 11, 68-72] For example, expression of *Ext1*,[11, 68] *Sdc1*, [11, 68, 69] *Gpc1*, [11, 69] and *Hspg2*[11, 68] is significantly increased within 2-4 weeks of surgical OA induction (Supplementary Table 1), in line with our findings here. Data on early changes in expression of sulfotransferases are variable, and early changes in *Hs6st1* were not reported. This may suggest that expression of this gene is stimulated once cartilage damage starts to escalate, but may also reflect differences between rodent post-traumatic OA and more variable human disease.

Age is a primary risk factor for the development of OA, and it is important to understand the cellular mechanisms that increase risk with age if we are to develop effective therapies to treat the disease. Previous studies have shown that HS sulfation patterns change with age in various tissues, including the aorta,[73] myocardium,[74] muscle stem cell niche[27] and brain,[75, 76] with concomitant changes in growth factor signalling. While our study was not powered to detect changes in HS disaccharide composition with age, we found that expression of *HS3ST2* in cartilage increased with age, in contrast to what has previously been reported in skin.[77] However, our observation is based on a low number of individuals (n = 11) as we had some missing values for *HS3ST2* expression. Further analysis of age-dependent changes in HS structure may identify changes that impair cartilage repair with age and so increase the risk of OA after injury.

Our analysis identified 6-O-sulfation as the primary HS motif that is altered in end-stage OA cartilage, validating it as a new target for potential therapeutic interventions. To understand the impact this change has on cartilage repair and OA progression, it will be necessary to carry out unbiased analyses of the 6-O-sulfate-binding proteome in normal and OA cartilage. Comparative mass spectrometry approaches have proved useful in examining the 3-O-sulfate-binding proteome in cultured cells,[64] and similar methods could be developed for cartilage analysis. Analysis of other joint tissues (e. g. bone, synovium, meniscus) and earlier stages of OA progression can also be expected to shed further light on the role of HS in adult joint homeostasis.

References

1. Sanchez-Adams J, Leddy HA, McNulty AL, O'Conor CJ, Guilak F: The mechanobiology of articular cartilage: bearing the burden of osteoarthritis. Curr Rheumatol Rep 2014, 16:451.
2. Vincent TL, McLean CJ, Full LE, Peston D, Saklatvala J: FGF-2 is bound to perlecan in the pericellular matrix of articular cartilage, where it acts as a chondrocyte mechanotransducer. Osteoarthritis Cartil 2007, 15:752-63.
3. Vincent TL, Hermansson MA, Hansen UN, Amis AA, Saklatvala J: Basic fibroblast growth factor mediates transduction of mechanical signals when articular cartilage is loaded. Arthritis Rheum 2004, 50:526-33.
4. Ori A, Wilkinson MC, Fernig DG: A systems biology approach for the investigation of the heparin/heparan sulfate interactome. J Biol Chem 2011, 286:19892-904.
5. Vincent TL: Targeting mechanotransduction pathways in osteoarthritis: a focus on the pericellular matrix. Curr Opin Pharmacol 2013, 13:449-54.
6. Tesche F, Miosge N: Perlecan in late stages of osteoarthritis of the human knee joint. . Osteoarthr Cartil 2004, 12:852-62.
7. Karlsson C, Dehne T, Lindahl A, Brittberg M, Pruss A, Sittinger M, Ringe J: Genome-wide expression profiling reveals new candidate genes associated with osteoarthritis. Osteoarthritis Cartilage 2010, 18:581-92.
8. Sato T, Konomi K, Yamasaki S, Aratani S, Tsuchimochi K, Yokouchi M, Masuko-Hongo K, Yagishita N, Nakamura H, Komiya S, Beppu M, Aoki H, Nishioka K, Nakajima T: Comparative analysis of gene expression profiles in intact and damaged regions of human osteoarthritic cartilage. Arthritis Rheum 2006, 54:808-17.
9. Loeser RF, Olex AL, McNulty MA, Carlson CS, Callahan MF, Ferguson CM, Chou J, Leng X, Fetrow JS: Microarray analysis reveals age-related differences in gene expression during the development of osteoarthritis in mice. Arthritis Rheum 2012, 64:705-17.

10. Salminen-Mankonen H, Säämänen a-M, Jalkanen M, Vuorio E, Pirilä L: Syndecan-1 expression is upregulated in degenerating articular cartilage in a transgenic mouse model for osteoarthritis. Scand J Rheumatol 2005, 34:469-74.
11. Gardiner MD, Vincent TL, Driscoll C, Burleigh A, Bou-Gharios G, Saklatvala J, Nagase H, Chanalaris A: Transcriptional analysis of micro-dissected articular cartilage in post-traumatic murine osteoarthritis. Osteoarthritis Cartil 2015, 23:616-28.
12. Barre P, Redinif F, Boumedienef K, Vielpeau C, Pujolf J: Semiquantitative reverse transcription-polymerase chain reaction analysis of syndecan-1 and -4 messages in cartilage and cultured chondrocytes from osteoarthritic joints. . Osteoarthr Cartil 2000, 8:34-43
13. Echtermeyer F, Bertrand J, Dreier R, Meinecke I, Neugebauer K, Fuerst M, Lee YJ, Song YW, Herzog C, Theilmeier G, Pap T: Syndecan-4 regulates ADAMTS-5 activation and cartilage breakdown in osteoarthritis. Nature Medicine 2009, 15:1072-6.
14. Guimond SE, Turnbull JE: Fibroblast growth factor receptor signalling is dictated by specific heparan sulfhate saccharides. Curr Biol 1999, 9:1343-6.
15. Shipp EL, Hsieh-Wilson LC: Profiling the sulfation specificities of glycosaminoglycan interactions with growth factors and chemotactic proteins using microarrays. Chem Biol 2007, 14:195-208.
16. Ashikari-Hada S, Habuchi H, Kariya Y, Itoh N, Reddi AH, Kimata K: Characterization of growth factor-binding structures in heparin/heparan sulfate using an octasaccharide library. J Biol Chem 2004, 279:12346-54.
17. Kreuger J, Kjellén L: Heparan sulfate biosynthesis: regulation and variability. J Histochem Cytochem 2012, 60:898-907.
18. Brickman Y, Nurcombe V, Gallagher J, Ford M, Turnbull J: Structural modification of FGF-binding HS at a determinative stage of neuroepithelial development. J Biol Chem 1998, 273:4350-9.
19. Kalus I, Rohn S, Puvirajesinghe TM, Guimond SE, Eyckerman-Kölln PJ, Ten Dam G, van Kuppevelt TH, Turnbull JE, Dierks T: Sulf1 and Sulf2 differentially modulate heparan sulfate proteoglycan sulfation during postnatal cerebellum development: evidence for neuroprotective and neurite outgrowth promoting functions. PLoS One 2015, 10:e0139853.

20. Thompson SM, Fernig DG, Jesudason EC, Losty PD, van de Westerlo EM, van Kuppevelt TH, Turnbull JE: Heparan sulfate phage display antibodies identify distinct epitopes with complex binding characteristics: insights into protein binding specificities. J Biol Chem 2009, 284:35621-31.
21. Buresh-Stiemke RA, Malinowski RL, Keil KP, Vezina CM, Oosterhof A, Van Kuppevelt TH, Marker PC: Distinct expression patterns of Sulf1 and Hs6st1 spatially regulate heparan sulfate sulfation during prostate development. Dev Dyn 2012, 241:2005-13.
22. Hosono-Fukao T, Ohtake-Niimi S, Hoshino H, Britschgi M, Akatsu H, Hossain M, Nishitsuji K, van Kuppevelt T, Kimata K, Michikawa M, Wyss-Coray T, Uchimura K: Heparan sulfate subdomains that are degraded by Sulf accumulate in cerebral amyloid ß plaques of Alzheimer's disease: evidence from mouse models and patients. Am J Pathol 2012, 180:2056-67.
23. Sepulveda-Diaz JE, Alavi Naini SM, Huynh MB, Ouidja MO, Yanicostas C, Chantepie S, Villares J, Lamari F, Jospin E, van Kuppevelt TH, Mensah-Nyagan AG, Raisman-Vozari R, Soussi-Yanicostas N, Papy-Garcia D: HS3ST2 expression is critical for the abnormal phosphorylation of tau in Alzheimer's disease-related tau pathology. Brain 2015, 138:1339-54.
24. Bernsen M, Smetsers T, van de Westerlo E, Ruiter D, Håkansson L, Gustafsson B, van Kuppevelt T, Krysander L, Rettrup B, Håkansson A: Heparan sulphate epitope-expression is associated with the inflammatory response in metastatic malignant melanoma. Cancer Immunol Immunother 2003, 52:780-3.
25. Wijnhoven T, Lensen J, Rops A, van der Vlag J, Kolset S, Bangstad H, Pfeffer P, van den Hoven M, Berden J, van den Heuvel L, van Kuppevelt T: Aberrant heparan sulfate profile in the human diabetic kidney offers new clues for therapeutic glycomimetics. Am J Kidney Dis 2006, 48:250-61.
26. Westergren-Thorsson G, Hedström U, Nybom A, Tykesson E, Åhrman E, Hornfelt M, Maccarana M, van Kuppevelt TH, Dellgren G, Wildt M, Zhou XH, Eriksson L, Bjermer L, Hallgren O: Increased deposition of glycosaminoglycans and altered structure of heparan sulfate in idiopathic pulmonary fibrosis. Int J Biochem Cell Biol 2017, 83:27-38.

552 27. Ghadiali RS, Guimond SE, Turnbull JE, Pisconti A: Dynamic changes in heparan sulfate during
553 muscle differentiation and ageing regulate myoblast cell fate and FGF2 signalling. Matrix Biol
554 2017, 59:54-68.
555 28. Skidmore MA, Guimond SE, Dumax-Vorzet AF, Atrih A, Yates EA, Turnbull JE: High sensitivity
556 separation and detection of heparan sulfate disaccharides. J Chromatogr A 2006, 1135:52-6.
557 29. Barbáchano A, Ordóñez-Morán P, García JM, Sánchez A, Pereira F, Larriba MJ, Martínez N,
558 Hernández J, Landolfi S, Bonilla F, Pálmer HG, Rojas JM, Muñoz A: SPROUTY-2 and E-cadherin
559 regulate reciprocally and dictate colon cancer cell tumourigenicity. Oncogene 2010, 29:4800-13.
560 30. Tenbaum S, Arqués O, Chicote I, Tenbaum S, Puig I, G. Palmer H: Standardized relative
561 quantification of immunofluorescence tissue staining. Protocol Exchange
562 2012:doi:10.1038/protex.2012.008.
563 31. Ismail HM, Miotla-Zarebska J, Troeberg L, Tang X, Stott B, Yamamoto K, Nagase H, Fosang AJ,
564 Vincent TL, Saklatvala J: JNK-2 controls aggrecan degradation in murine articular cartilage and
565 the development of experimental osteoarthritis. Arthritis Rheumatol 2016, 68:1165-71.
566 32. Rani Das K, M Rahmatullah Imon AH, M Rahmatullah AH: A brief review of tests for normality.
567 Am J Theor Appl Stat 2016, 5.
568 33. Benjamini Y, Krieger AM, Yekutieli D: Adaptive linear step-up procedures that control the false
569 discovery rate. Biometrika 2006, 93:491-507.
570 34. Iozzo RV, Cohen IR, Grassel S, Murdoch AD: The biology of perlecan: the multifaceted heparan
571 sulphate proteoglycan of basement membranes and pericellular matrices. Biochem J 1994, 302:625-
572 39.
573 35. Sakamoto S, Goldhaber P, Glimcher M: Mouse bone collagenase. The effect of heparin on the
574 amount of enzyme released in tissue culture and on the activity of the enzyme. Calcif Tissue Res
575 1973, 12:247-58.
576 36. Gao G, Plaas A, Thompson V, Jin S, Zuo F, Sandy J: ADAMTS4 (aggrecanase-1) activation on the
577 cell surface involves C-terminal cleavage by glycosylphosphatidyl inositol-anchored membrane
578 type 4-matrix metalloproteinase and binding of the activated proteinase to chondroitin sulfate and
579 heparan sulfate on syndecan-1. J Biol Chem 2004, 279:10042-51.

580 37. Zeng W, Corcoran C, Collins-Racie L, Lavallie E, Morris E, Flannery C: Glycosaminoglycan-
581 binding properties and aggrecanase activities of truncated ADAMTSs: comparative analyses with
582 ADAMTS-5, -9, -16 and -18. Biochim Biophys Acta 2006, 1760:517-24.
583 38. Koziel L, Kunath M, Kelly O, Vortkamp A: Ext1-dependent heparan sulfate regulates the range of
584 Ihh signaling during endochondral ossification. . Dev Cell 2004, 6:801-13.
585 39. Pacifici M: The pathogenic roles of heparan sulfate deficiency in hereditary multiple exostoses.
586 Matrix Biol 2017, In press.
587 40. Sun MM, Beier F: Chondrocyte hypertrophy in skeletal development, growth, and disease. Birth
588 Defects Res C Embryo Today 2014, 102:74-82.
589 41. Busse-Wicher M, Wicher KB, Kusche-Gullberg M: The exostosin family: proteins with many
590 functions. Matrix Biol 2014, 35:25-33.
591 42. Notarangelo LD: Expanding the spectrum of skeletal dysplasia with immunodeficiency: a
592 commentary on identification of biallelic EXTL3 mutations in a novel type of spondylo-epi-
593 metaphyseal dysplasia. J Hum Genet 2017, 62:737-8.
594 43. Habuchi H, Tanaka M, Habuchi O, Yoshida K, Suzuki H, Ban K, K. K: The occurrence of three
595 isoforms of heparan sulfate 6-O-sulfotransferase having different specificities for hexuronic acid
596 adjacent to the targeted N-sulfoglucosamine. J Biol Chem 2000, 275:2859-6.
597 44. Lu J, Auduong L, White ES, Yue X: Up-regulation of heparan sulfate 6-O-sulfation in idiopathic
598 pulmonary fibrosis. Am J Respir Cell Mol Biol 2014, 50:106-14.
599 45. Alhasan AA, Spielhofer J, Kusche-Gullberg M, Kirby JA, Ali S: Role of 6-O-sulfated heparan
600 sulfate in chronic renal fibrosis. J Biol Chem 2014, 289:20295-306.
601 46. Ferreras C, Rushton G, Cole CL, Babur M, Telfer BA, van Kuppevelt TH, Gardiner JM, Williams
602 KJ, Jayson GC, Avizienyte E: Endothelial heparan sulfate 6-O-sulfation levels regulate angiogenic
603 responses of endothelial cells to fibroblast growth factor 2 and vascular endothelial growth factor.
604 J Biol Chem 2012, 287:36132-46.
605 47. Waaijer CJ, de Andrea CE, Hamilton A, van Oosterwijk JG, Stringer SE, Bovée JV: Cartilage
606 tumour progression is characterized by an increased expression of heparan sulphate 6O-sulphation-
607 modifying enzymes. Virchows Arch 2012, 461:475-81.

608 48. Pellegrini L, Burke DF, von Delft F, Mulloy B, Blundell TL: Crystal structure of fibroblast growth
609 factor receptor ectodomain bound to ligand and heparin. Nature 2000, 407:1029-34.
610 49. Schlessinger J, Plotnikov AN, Ibrahimi OA, Eliseenkova AV, Yeh BK, Yayon A, Linhardt RJ,
611 Mohammadi M: Crystal structure of a ternary FGF-FGFR-heparin complex reveals a dual role for
612 heparin in FGFR binding and dimerization. Mol Cell 2000, 6:743-50.
613 50. Pye D, Vives R, Turnbull J, Hyde P, Gallagher J: Heparan sulfate oligosaccharides require 6-O-
614 sulfation for promotion of basic fibroblast growth factor mitogenic activity. J Biol Chem 1998,
615 273:22936-42.
616 51. Jemth P, Kreuger J, Kusche-Gullberg M, Sturiale L, Giménez-Gallego G, Lindahl U: Biosynthetic
617 oligosaccharide libraries for identification of protein-binding heparan sulfate motifs. Exploring the
618 structural diversity by screening for fibroblast growth factor (FGF)1 and FGF2 binding. J Biol
619 Chem 2002, 277:30567-73.
620 52. El Masri R, Seffouh A, Lortat-Jacob H, Vivès RR: The "in and out" of glucosamine 6-O-sulfation:
621 the 6th sense of heparan sulfate. Glycoconj J 2017, 34:285-98.
622 53. Lyon M, Rushton G, Gallagher J: The interaction of the transforming growth factor-betas with
623 heparin/heparan sulfate is isoform-specific. J Biol Chem 1997, 272:18000-6.
624 54. Yue X, Li X, Nguyen HT, Chin DR, Sullivan DE, Lasky JA: Transforming growth factor-beta1
625 induces heparan sulfate 6-O-endosulfatase 1 expression in vitro and in vivo. J Biol Chem 2008,
626 283:20397-407.
627 55. Ai X, Do AT, Lozynska O, Kusche-Gullberg M, Lindahl U, Emerson CPJ: QSulf1 remodels the 6-
628 O sulfation states of cell surface heparan sulfate proteoglycans to promote Wnt signaling. J Cell
629 Biol 2003, 162:341-51.
630 56. Dhoot G, Gustafsson M, Ai X, Sun W, Standiford D, Emerson CJ: Regulation of Wnt signaling and
631 embryo patterning by an extracellular sulfatase. Science 2001, 293:1663-6.
632 57. Viviano BL, Paine-Saunders S, Gasiunas N, Gallagher J, Saunders S: Domain-specific modification
633 of heparan sulfate by Qsulf1 modulates the binding of the bone morphogenetic protein antagonist
634 Noggin. J Biol Chem 2004, 279:5604-11.

635 58. Otsuki S, Hanson SR, Miyaki S, Grogan SP, Kinoshita M, Asahara H, Wong C-H, Lotz MK:
636 Extracellular sulfatases support cartilage homeostasis by regulating BMP and FGF signaling
637 pathways. Proc Natl Acad Sci U S A 2010, 107:10202-7.
638 59. Morimoto-Tomita M, Uchimura K, Werb Z, Hemmerich S, Rosen S: Cloning and characterization
639 of two extracellular heparin-degrading endosulfatases in mice and humans. J Biol Chem 2002,
640 277:49175-85.
641 60. Otsuki S, Taniguchi N, Grogan SP, D'Lima D, Kinoshita M, Lotz M: Expression of novel
642 extracellular sulfatases Sulf-1 and Sulf-2 in normal and osteoarthritic articular cartilage. Arthritis
643 Res Ther 2008, 10:R61.
644 61. Bateman JF, Rowley L, Belluoccio D, Chan B, Bell K, Fosang AJ, Little CB: Transcriptomics of
645 wild-type mice and mice lacking ADAMTS-5 activity identifies genes involved in osteoarthritis
646 initiation and cartilage destruction. Arthritis Rheum 2013, 65:1547-60.
647 62. Otsuki S, Murakami T, Okamoto Y, Hoshiyama Y, Oda S, Neo M: Suppression of cartilage
648 degeneration by intra-articular injection of heparan sulfate 6-O endosulfatase in a mouse
649 osteoarthritis model. Histol Histopathol 2017, 32:725-33.
650 63. Huang Y, Mao Y, Zong C, Lin C, Boons GJ, Zaia J: Discovery of a heparan sulfate 3-O-sulfation
651 specific peeling reaction. Anal Chem 2015, 87:592-600.
652 64. Thacker BE, Seamen E, Lawrence R, Parker MW, Xu Y, Liu J, Vander Kooi CW, Esko JD:
653 Expanding the 3-O-sulfate proteome - enhanced binding of neuropilin-1 to 3-O-sulfated heparan
654 sulfate modulates its activity. ACS Chem Biol 2016, 11:971-80.
655 65. Pfander D, Swoboda B, Kirsch T: Expression of early and late differentiation markers (proliferating
656 cell nuclear antigen, syndecan-3, annexin VI, and alkaline phosphatase) by human osteoarthritic
657 chondrocytes. Am J Pathol 2001, 159:1777-83.
658 66. Eldridge S, Nalesso G, Ismail H, Vicente-Greco K, Kabouridis P, Ramachandran M, Niemeier A,
659 Herz J, Pitzalis C, Perretti M, Dell'Accio F: Agrin mediates chondrocyte homeostasis and requires
660 both LRP4 and α-dystroglycan to enhance cartilage formation in vitro and in vivo. Ann Rheym Dis
661 2016, 75:1228-35.

662 67. Tang X, Muhammad H, McClean C, Zarebska J, Flemming J, Didangelos A, Önnerfjord P, Leask
663 A, Saklatvala J, Vincent TL: Connective tissus growth factor (CTGF) contributes to joint
664 homeostasis and osteoarthritis severity by controlling the matrix sequestration and activation of
665 latent TGFβ. Ann Rheum Dis 2018, 77:1372-80.
666 68. Loeser RF, Olex AL, McNulty MA, Carlson CS, Callahan M, Ferguson C, Fetrow JS: Disease
667 progression and phasic changes in gene expression in a mouse model of osteoarthritis. PLoS One
668 2013, 8:e54633.
669 69. Appleton CTG, Pitelka V, Henry J, Beier F: Global analyses of gene expression in early
670 experimental osteoarthritis. Arthritis Rheum 2007, 56:1854-68.
671 70. Geyer M, Grassel S, Straub RH, Schett G, Dinser R, Grifka J, Gay S, Neumann E, Muller-Ladner
672 U: Differential transcriptome analysis of intraarticular lesional vs intact cartilage reveals new
673 candidate genes in osteoarthritis pathophysiology. Osteoarthritis Cartilage 2009, 17:328-35.
674 71. Dunn SL, Soul J, Anand S, Schwartz JM, Boot-Handford RP, Hardingham TE: Gene expression
675 changes in damaged osteoarthritic cartilage identify a signature of non-chondrogenic and
676 mechanical responses. Osteoarthritis Cartilage 2016 24:1431-40.
677 72. Snelling S, Rout R, Davidson R, Clark I, Carr A, Hulley PA, Price AJ: A gene expression study of
678 normal and damaged cartilage in anteromedial gonarthrosis, a phenotype of osteoarthritis.
679 Osteoarthritis Cartilage 2014, 22:334-43.
680 73. Feyzi E, Saldeen T, Larsson E, Lindahl U, Salmivirta M: Age-dependent modulation of heparan
681 sulfate structure and function. J Biol Chem 1998, 273:13395-8.
682 74. Huynh MB, Morin C, Carpentier G, Garcia-Filipe S, Talhas-Perret S, Barbier-Chassefière V, van
683 Kuppevelt TH, Martelly I, Albanese P, Papy-Garcia D: Age-related changes in rat myocardium
684 involve altered capacities of glycosaminoglycans to potentiate growth factor functions and heparan
685 sulfate-altered sulfation. J Biol Chem 2012, 287:11363-73.
686 75. Huynh MB, Villares J, Díaz JE, Christiaans S, Carpentier G, Ouidja MO, Sissoeff L, Raisman-
687 Vozari R, Papy-Garcia D: Glycosaminoglycans from aged human hippocampus have altered
688 capacities to regulate trophic factors activities but not Aβ42 peptide toxicity. Neurobiol Aging
689 2012, 33:1005.e11-22.

690 76. Yamada T, Kerever A, Yoshimura Y, Suzuki Y, Nonaka R, Higashi K, Toida T, Mercier F,
691 Arikawa-Hirasawa E: Heparan sulfate alterations in extracellular matrix structures and fibroblast
692 growth factor-2 signaling impairment in the aged neurogenic niche. J Neurochem 2017, 142:534-
693 44.
694 77. Glass D, Viñuela A, Davies MN, Ramasamy A, Parts L, Knowles D, Brown AA, Hedman ÅK,
695 Small KS, Buil A, Grundberg E, Nica AC, Meglio P, Nestle FO, Ryten M, Durbin R, McCarthy
696 MI, Deloukas P, Dermitzakis ET, Weale ME, Bataille V, Spector TD: Gene expression changes
697 with age in skin, adipose tissue, blood and brain. Genome Biol 2013, 14:R75.

698 **Table 1:** Primer/probe sets used on custom-designed Taqman low density arrays.

699

Gene name	Primer/probe set
Chain elongation	
EXT1	Hs00609162_m1
EXT2	Hs00181158_m1
EXTL1	Hs00184929_m1
EXTL2	Hs01018237_m1
EXTL3	Hs00918601_m1
N-deacetylase/ N-sulfotransferases	
NDST1	Hs00925442_m1
NDST2	Hs00234335_m1
NDST3	Hs01128584_m1
NDST4	Hs00224024_m1
Glucuronyl C5-epimerase	
GLCE	Hs00392011_m1
2-O-sulfotransferase	
HS2ST1	Hs00202138_m1
3-O-sulfotransferases	
HS3ST1	Hs00245421_s1
HS3ST2	Hs00428644_m1
HS3ST3A1	Hs00925624_s1
HS3ST3B1	Hs00797512_s1
HS3ST4	Hs00901124_s1
HS3ST5	Hs00999394_m1
HS3ST6	Hs03007244_m1
6-O-sulfotransferases	
HS6ST1	Hs00757137_m1
HS6ST2	Hs02925656_m1
HS6ST3	Hs00542178_m1
Editing enzymes	
HSPE	Hs00935036_m1
HSPE2	Hs00222435_m1
SULF1	Hs00290918_m1
SULF2	Hs01016476_m1
Core proteins	
AGRN	Hs00394748_m1
GPC1	Hs00892476_m1
GPC2	Hs00415099_m1
GPC3	Hs01018936_m1
GPC4	Hs00155059_m1
GPC5	Hs00270114_m1
GPC6	Hs00170677_m1
HSPG2	Hs00194179_m1
SDC1	Hs00896423_m1
SDC2	Hs00299807_m1
SDC3	Hs01568665_m1
SDC4	Hs00161617_m1
TGFBR3	Hs01114253_m1
Normalising genes	
18S	Hs99999901_s1
RPLP0	Hs99999902_m1
GAPDH	Hs99999905_m1

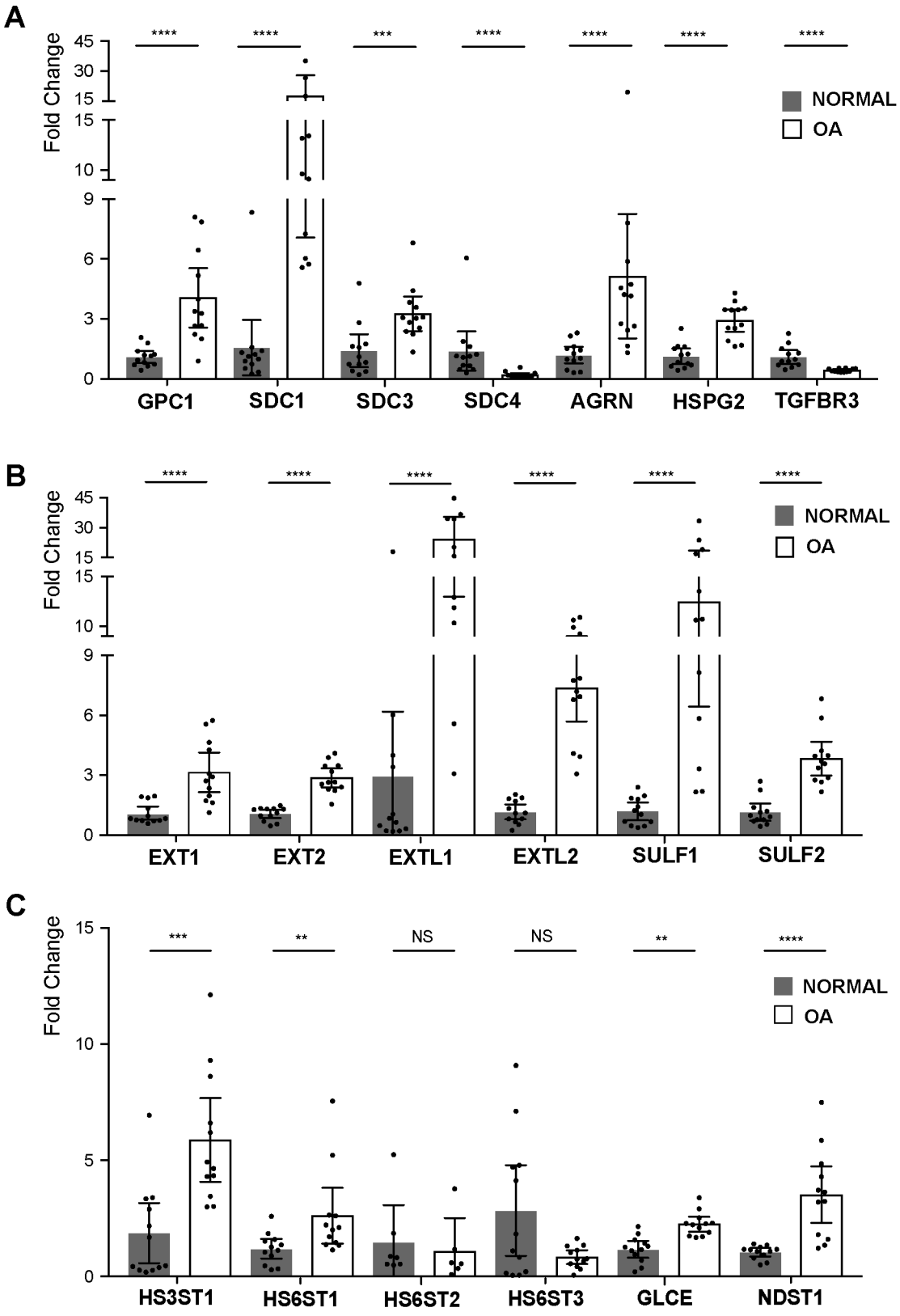

700

701 **Figure 1.** Changes in HS-related gene expression in human OA cartilage. Expression of HS-associated

702 genes in normal and OA cartilage (n = 12 per group) was analysed using Taqman low-density arrays.

703 Fold changes in expression were determined by the ΔΔCt method against the average of the normal

704 samples. **A:** Fold changes in expression of HS core protein genes. **B:** Fold changes in expression of HS
705 chain elongation and sulfatase genes. **C:** Fold changes in expression of sulfotransferase genes. Error
706 bars represent 95% of confidence intervals of the mean. ** $q < 0.01$, *** $q < 0.001$, **** $q < 0.0001$ by
707 BKY corrected multiple t-test.

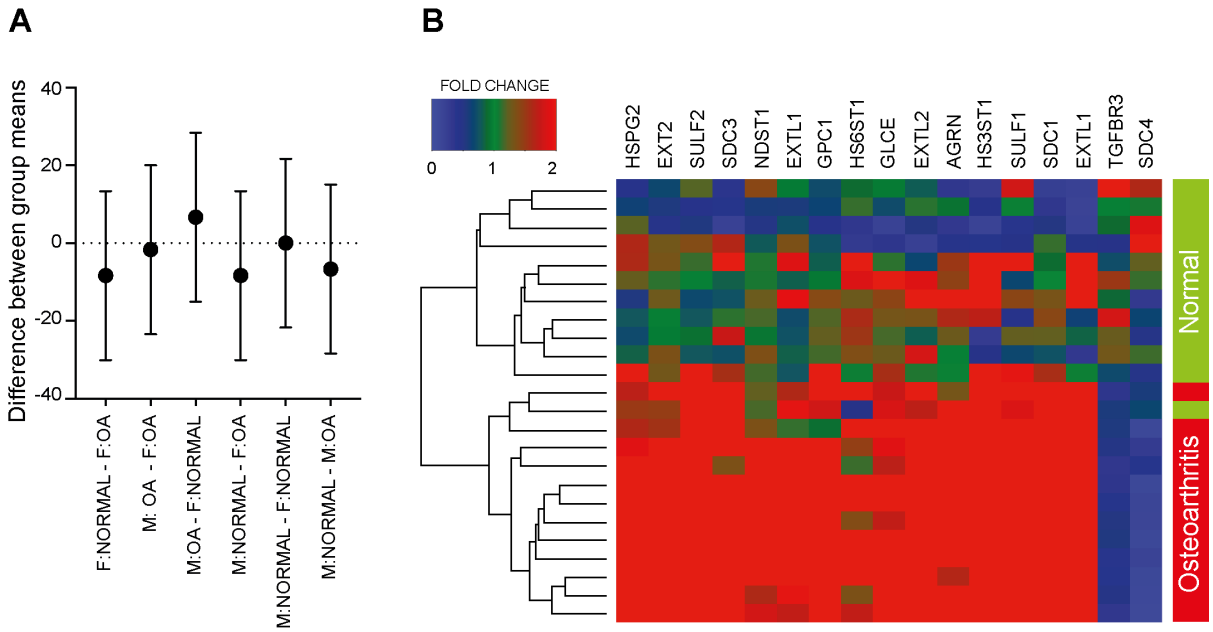

Figure 2. Expression of HS-associated genes is altered in OA cartilage. **A:** Forest plot showing there was no significant difference between the ages and genders of normal (n = 12) and OA (n = 12) cartilage donors used for gene expression analysis. M, male; F, female. Bars show 95% confidence intervals of the mean, dotted line shows Y=0. **B:** Expression of HS-associated genes in normal and OA cartilage was analysed using Taqman low-density arrays. Fold change in expression were determined by the ΔΔCt method against the average of the normal samples. The heatmap shows only those HS-associated genes whose expression was significantly different in the two groups (n = 12 for each group; BKY corrected multiple t-test; q-value < 0.05), with increased expression in OA shown in red, reduced expression shown in blue, and no change indicated in green. Cluster analysis based on the expression levels of significantly regulated genes separated the samples into two clusters, with the first cluster containing all of the OA samples and one of the normal samples, and the second cluster containing the remaining normal samples.

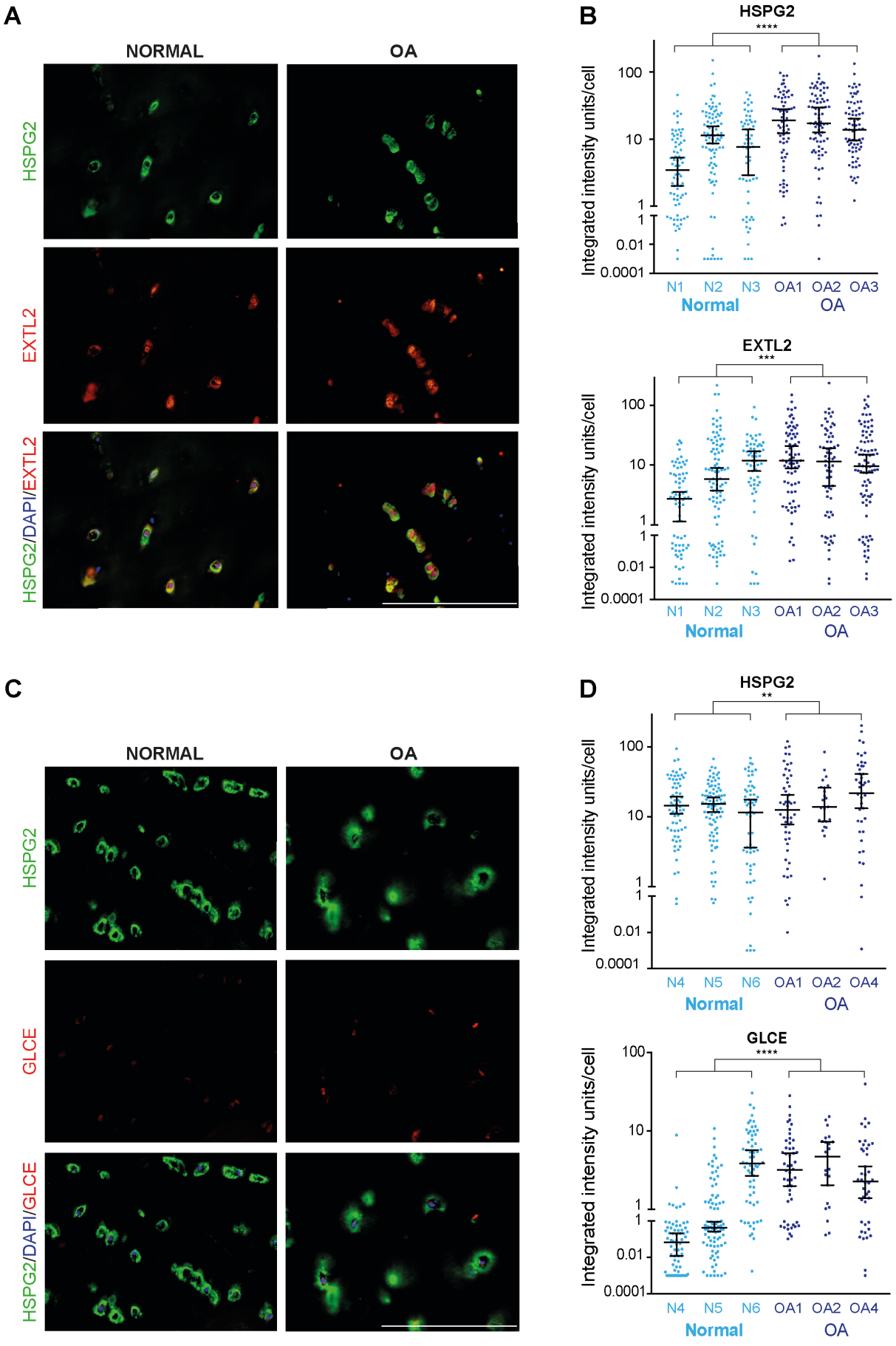
A
NORMAL
OA
HSPG2
EXTL2
HSPG2/DAPI/EXTL2
B
HSPG2
****
Integrated intensity units/cell
100
10
1
1
0.01
0.0001
N1 N2 N3 OA1 OA2 OA3
Normal
OA
EXTL2
***
Integrated intensity units/cell
100
10
1
1
0.01
0.0001
N1 N2 N3 OA1 OA2 OA3
Normal
OA
C
NORMAL
OA
HSPG2
GLCE
HSPG2/DAPI/GLCE
D
HSPG2
**
Integrated intensity units/cell
100
10
1
1
0.01
0.0001
N4 N5 N6 OA1 OA2 OA4
Normal
OA
GLCE
****
Integrated intensity units/cell
100
10
1
1
0.01
0.0001
N4 N5 N6 OA1 OA2 OA4
Normal
OA

721

Figure 3. Expression of HSPG2, EXTL2 and GLCE is increased in human OA cartilage. **A:** Representative images showing expression of HSPG2 and EXLT2 in human normal and OA cartilage. **B:** Expression of HSPG2 and EXLT2 was semi-quantitatively evaluated in 3 normal donors (N1, N2 and N3) and 3 OA donors (OA1, OA2 and OA3), with each dot representing integrated fluorescence intensity per single cell, calculated from at least 6 random fields of view on 3 sections per donor. For each donor, the median fluorescence intensity with 95% confidence intervals of the mean are shown. **C:** Representative images showing expression of HSPG2 and GLCE in human normal and OA cartilage. **D:** Expression of HSPG2 and GLCE was semi-quantitatively evaluated in 3 normal donors (N4, N5 and N6) and 3 OA donors (OA1, OA2 and OA4) as described in **B**. ** $P < 0.01$, *** $P < 0.001$, **** $P < 0.0001$ by Kolmogorov-Smirnov test. Scale bar = 260 μm.

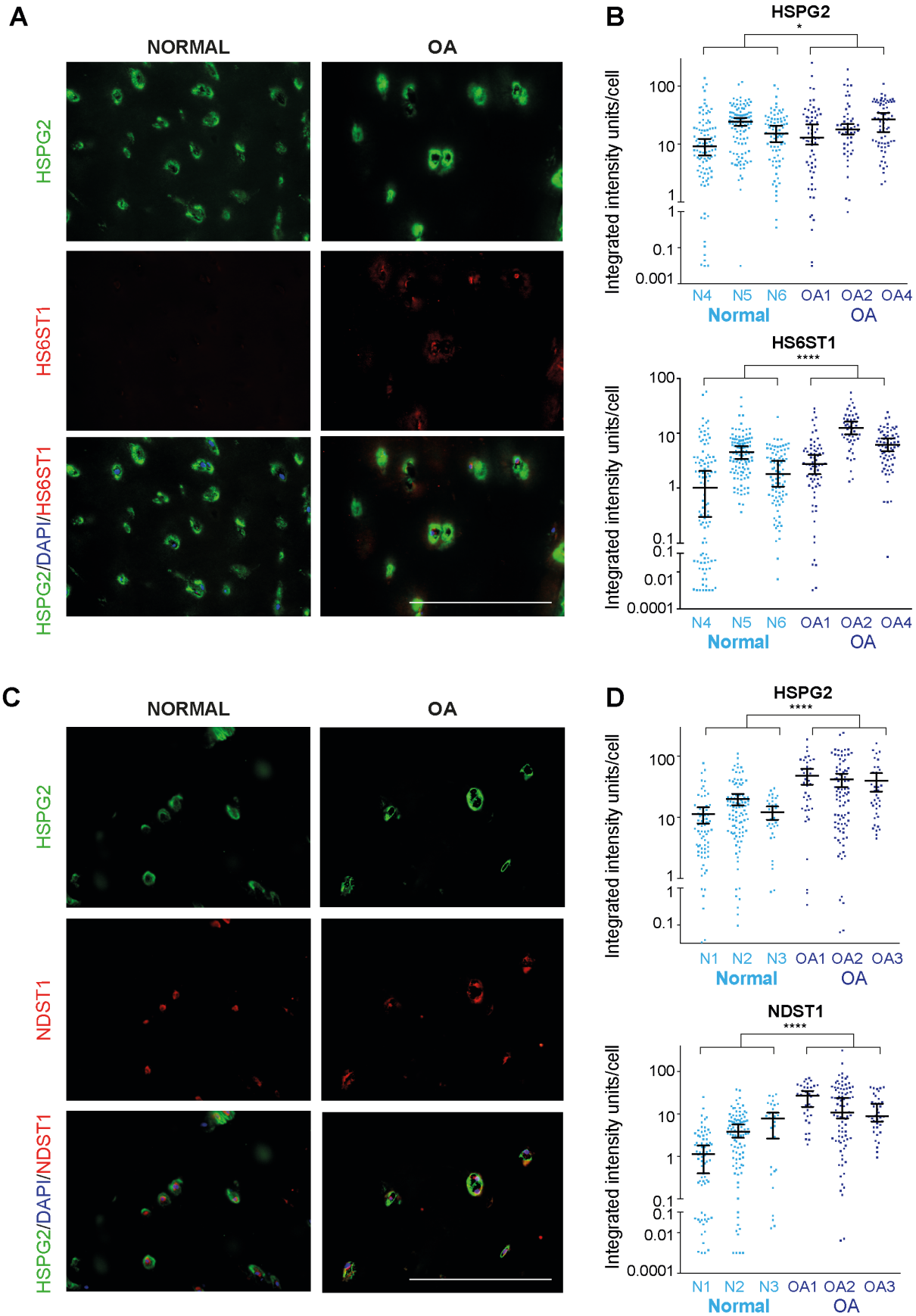
A
NORMAL
OA
HSPG2
HS6ST1
HSPG2/DAPI/HS6ST1
B
HSPG2
*
Integrated intensity units/cell
100
10
1
1
0.1
0.001
N4 N5 N6 OA1 OA2 OA4
Normal
OA
HS6ST1
****
Integrated intensity units/cell
100
10
1
0.1
0.1
0.01
0.0001
N4 N5 N6 OA1 OA2 OA4
Normal
OA
C
NORMAL
OA
HSPG2
NDST1
HSPG2/DAPI/NDST1
D
HSPG2
****
Integrated intensity units/cell
100
10
1
1
0.1
N1 N2 N3 OA1 OA2 OA3
Normal
OA
NDST1
****
Integrated intensity units/cell
100
10
1
0.1
0.1
0.01
0.0001
N1 N2 N3 OA1 OA2 OA3
Normal
OA

732

Figure 4. Expression of HSPG2, HS6ST1 and NDST1 is increased in human OA cartilage. **A:** Representative images showing expression of HSPG2 and HS6ST1 in human normal and OA cartilage. **B:** Expression of HSPG2 and HS6ST1 was semi-quantitatively evaluated in 3 normal donors (N4, N5 and N6) and 3 OA donors (OA1, OA2 and OA4), with each dot representing integrated fluorescence intensity per single cell, calculated from at least 6 random fields of view on 3 sections per donor. For each donor, the median fluorescence intensity with 95% confidence intervals of the mean are shown. **C:** Representative images showing expression of HSPG2 and NDST1 in human normal and OA cartilage. **D:** Expression of HSPG2 and NDST1 was semi-quantitatively evaluated in 3 normal donors (N1, N2 and N3) and 3 OA donors (OA1, OA2 and OA3) as described in **B**. *$P < 0.05$, **** $P < 0.0001$ by Kolmogorov-Smirnov test. Scale bar = 260 μm.

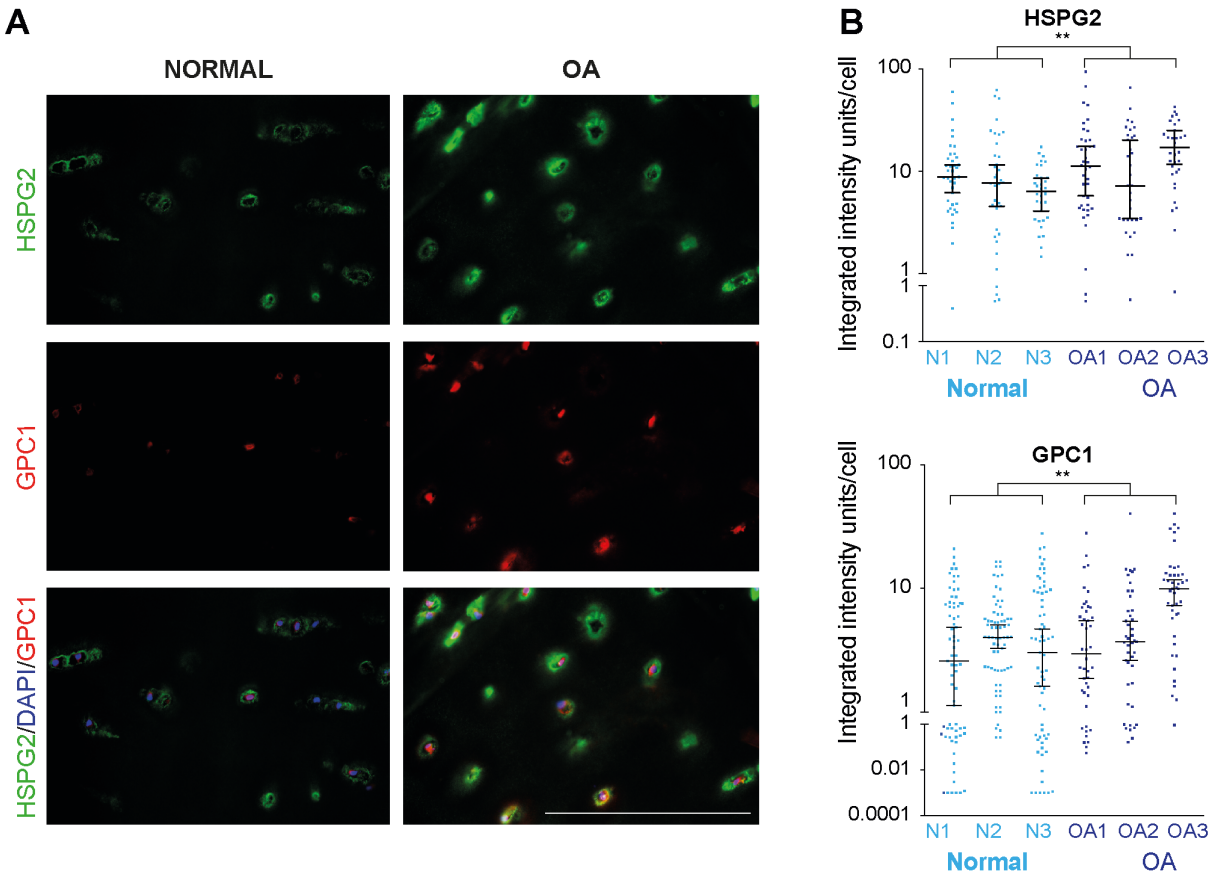

743

744 **Figure 5.** Expression of HSPG2 and glypican 1 (GPC1) is increased in human OA cartilage. **A:**
745 Representative images showing expression of HSPG2 and GPC1 in human normal and OA cartilage.
746 **B:** Expression of HSPG2 and GPC1 was semi-quantitatively evaluated in 3 normal donors (N1, N2 and
747 N3) and 3 OA donors (OA1, OA2 and OA3), with each dot representing integrated fluorescence
748 intensity per single cell, calculated from at least 6 random fields of view on 3 sections per donor. For
749 each donor, the median fluorescence intensity with 95% confidence intervals of the mean are shown.
750 ** $P < 0.01$ by Kolmogorov-Smirnov test. Scale bar = 260 µm.

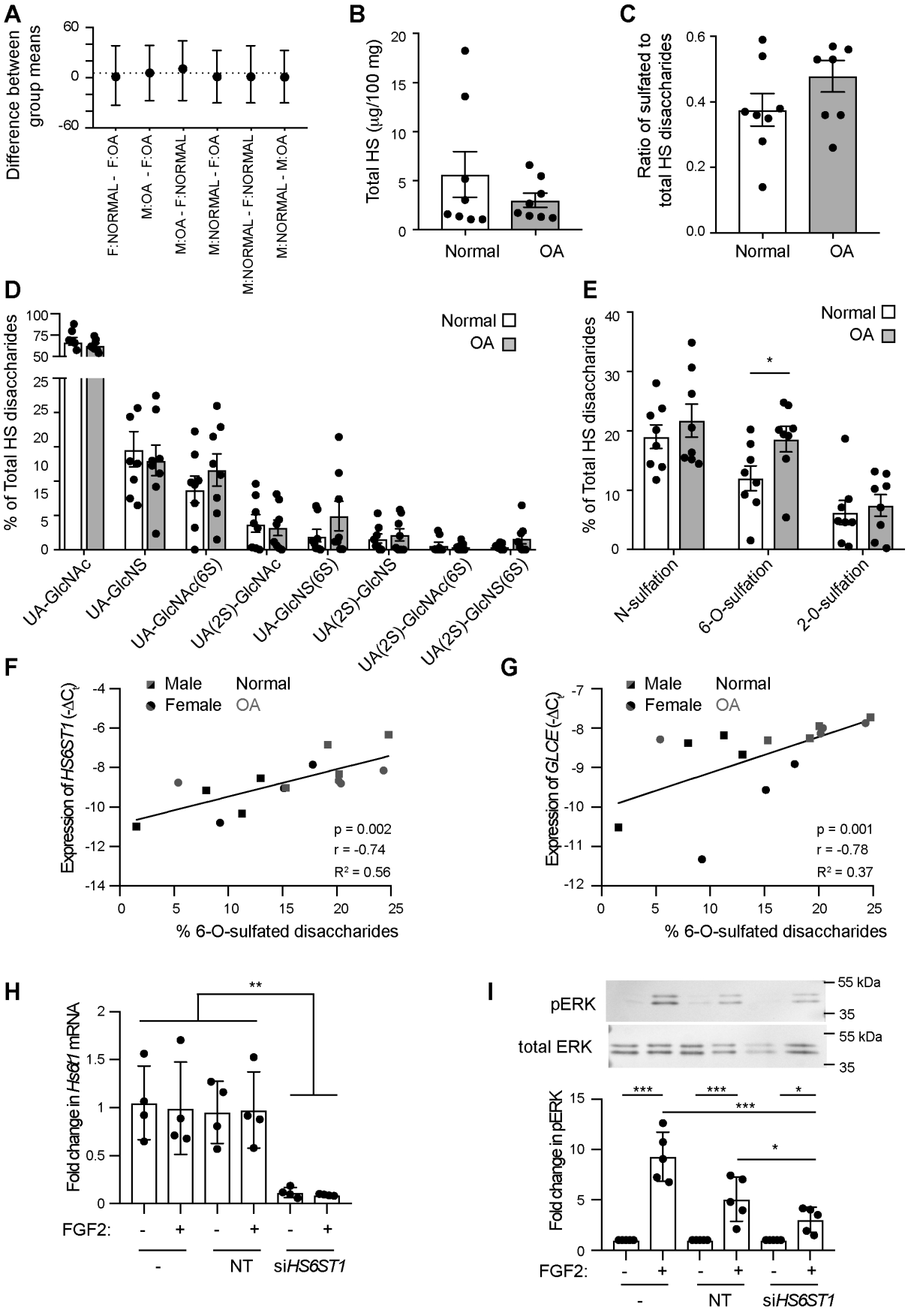

751

752 **Figure 6.** 6-O-sulfation is increased in OA cartilage. HS was isolated from normal (n = 8) and OA (n

= 8) cartilage and its composition analyzed by disaccharide analysis. **A:** Forest plot showing there was no significant difference between the ages and genders of normal (n = 8) and OA (n = 8) cartilage donors used for HS analysis. M, male; F, female. Bars show 95% confidence intervals of the mean , dotted line shows Y=0. **B:** The total amount of HS in OA cartilage was not statistically different from that in normal cartilage. **C:** The ratio of sulfated to total HS was not statistically different between the two groups of samples. **D:** Abundance of individual disaccharide species was not significantly different in normal and OA cartilage. GlcNAc, N-acetyl glucosamine; GlcNS, *N*-sulfoglucosamine; UA, uronic acid; 2S, 2-O-sulfate; 6S, 6-O-sulfate. **E:** 6-O-sulfated HS disaccharides were more abundant in OA cartilage, while levels of N- and 2-O-sulfation were not significantly altered. **F:** The level of 6-O-sulfation in donor cartilage correlated with expression of HS6ST1 (n = 15, normal cartilage shown in black, OA cartilage in grey, males as squares, female samples as circles). **G:** The level of 6-O-sulfation in donor cartilage also correlated with expression of GLCE (n = 15, normal cartilage shown in black, OA cartilage in grey, males as squares, female samples as circles). **H**: Expression of *HS6ST1* in primary OA chondrocytes was silenced using siRNA (n = 5 donors). NT, transfected with non-targeting siRNA. **I**: Silencing of *HS6ST1* in primary OA chondrocytes reduced phosphorylation of ERK in response to FGF2 (20 ng/ml, 10 min)(n = 5 donors). **P* < 0.05, ** P <0.01, *** P < 0.001, multiple t-tests BKY corrected.

Supplementary Table 1: Changes in expression of HS biosynthesis and modifying genes, adapted from published murine and human transcriptome datasets. Gardiner[11] and Loeser[68] examined changes in gene expression after surgical induction of OA in mice by destabilisation of the medial meniscus (DMM), while Appleton[69] used the more severe ACLT (anterior cruciate ligament transection) model in rats. For the human studies, late-stage damaged OA cartilage was compared to normal cartilage (Karlsson[7] and Sato[8]) or to macroscopically intact cartilage from the same OA joint (Geyer,[70] Dunn,[71] and Snelling[72]).

	Rodent – early OA			**Human – late stage OA**				
	Gardiner	Appleton	Loeser	Karlsson	Geyer	Sato	Dunn	Snelling
	2 weeks post DMM	4 weeks post ACLT	4 weeks post DMM	OA vs normal	OA lesion vs intact	OA vs normal	OA lesion vs intact	OA lesion vs intact
Up in OA	*Ext1*		*Ext1*	*EXTL2*	*EXTL2*			
	Sdc1	*Sdc1*	*Sdc1*					
	Sdc2	*Sdc2*	*Sdc4*					
	Gpc1	*Gpc1*				*GPC5*	*GPC4*	
		Gpc2	*Gpc6*					
	Hspg2		*Hspg2*	*HPGS2*		*HPGS2*		
	Sulf2		*Sulf1*	*SULF1*				
	Hs2st1						*HS3ST2*	*HS3ST3A1*
							HSPE2	
Down in OA	*Extl1*						*EXTL1*	
	Sdc4						*SDC3*	*SDC3*
							GPC5	*GPC4*
					GPC6		*GPC6*	
	Tgfbr3				*TGFBR3*			
	Hs3st3a1	*Hs3st1*		*HS3ST3A1*				
	Hs3st3b1			*HS3ST3B1*				
								SULF1